ISSN 0031-918X, The Physics of Metals and Metallography, 2006, Vol. 102, Suppl. 1, pp. S2–S7. © Pleiades Publishing, Inc., 2006.

MAGNETIC PARTICLES AND NANOCRYSTALLINE MATERIALS

CHAPTER 11

Magnetic Nanoparticles in Oxide Glasses[1]

I. S. Edelman[a], R. D. Ivantsov[a], I. G. Vasil'eva[b], A. D. Vasil'ev[a], O. A. Bayukov[a], O. S. Ivanova[a], D. E. Prokof'ev[a], S. A. Stepanov[c], E. E. Kornilova[c], T. V. Zarubina[c], V. V. Malakhov[d], and V. A. Zaikovskii[d]

[a] *Kirensky Institute of Physics, Siberian Division, Russian Academy of Sciences, Krasnoyarsk, 660036, Russia*

[b] *Institute of Inorganic Chemistry, Siberian Division, Russian Academy of Sciences, Novosibirsk, 630090, Russia*

[c] *Vavilov Optical State Institute, S. Petersburg, 192371, Russia*

[d] *Boreskov Institute of Catalysis, Siberian Division, Russian Academy of Sciences, Novosibirsk, 630090, Russia*

Abstract—Unique properties of the potassium–aluminum–boron glasses doped with low concentrations of MnO and Fe_2O_3 to make them magnetically ordered and optically transparent in the IR and visible ranges are due to the formation of nanoparticles of a cubic ferrite. Assembling and properties of nanosized ferrite particles in the glasses have been investigated by X-ray diffraction, differential dissolution analysis, high-resolution transmission electron microscopy, Mössbauer spectroscopy, magnetic measurements, and magnetooptical Faraday effect. It was shown that the ferrite particles vary highly in size, shape, stoichiometry, structural perfection, and space distribution depending on the preparation conditions. A correlation between the characteristics of nanostructured ferrite particles and magnetic properties of glasses has been established.

PACS numbers: 75.75.+a, 75.50.Lk

DOI: 10.1134/S0031918X0614002X

1. INTRODUCTION

Unique magnetic properties of borate glasses doped with small amounts of Mn and Fe oxides were observed for the fist time in 1974 [1]. Later, the problem of clustering of the paramagnetic ions in borate glasses has been raised in [2, 3]. The magnetic properties of the glasses were explained by the formation of nanoparticles of a magnetic ferrite in the amorphous matrix after a detailed study of the glasses by X-ray diffraction, Mössbauer and optical spectroscopy, magnetic and Faraday-effect measurements (see, e.g., [4, 5]). However, the specific properties of nanocrystalline materials are determined not only by the size of individual particles but also by their structure, lattice parameters, composition, crystalline perfection, size-distribution, and level of coalescence [5, 6]. The necessity of measurements of all these parameters makes the characterization of nanomaterials more complicated. The aim of this work was to find techniques adequate to studying the nanostructure of ferrite particles in K_2O–Al_2O_3–B_2O_3 glasses. A systematic analysis of several glasses was carried out via a combined study by X-ray diffraction (XRD), differential dissolution analysis (DDA), high-resolution transmission electron microscopy (HRTEM), Mössbauer spectroscopy (MS), magnetooptical Faraday rotation effect (FR), and magnetic measurements. Based on the experimental results, effects of the assembling of the ferrite nanoparticles and of their characteristics on the properties of the borate glasses have been considered.

2. EXPERIMENTAL

Glass samples were synthesized using the technology described in detail in [1–4]. Three glasses (1, 2, and 3) of the basic composition $22.5K_2O$–$22.5Al_2O_3$–$55B_2O_3$ were prepared for the present investigation. The amounts of the paramagnetic oxides MnO + Fe_2O_3 were taken in glasses 1, 2, and 3 in wt % as 1.0 + 1.5, 2.0 + 3.0, and 1.5 + 1.5, respectively. At the first stage, the synthesis conditions were the same for all samples. At the last stage, an additional heat treatment was made under different conditions, namely, at temperatures 460 and 600°C for glass 1, and 560 and 600°C for glass 2. Glass 3 was treated only at 560°C.

Structural analysis was performed by XRD. The XRD patterns had been collected in the range of 2Θ = 5°–60° using Cu $K\alpha$ radiation (1.5406 Å) and a D8 ADVANCE (Bruker) diffractometer. Phase chemical analysis was performed by the DDA technique [7]. In this case, the phase identification is based on the determination of the stoichiometric composition of the phases under conditions where only a single phase is dissolved from the mixture. An atomic-emission spectrometer with an inductively coupled plasma (ICP AES) was used in the DDA equipment as a detec-

[1] The text was submitted by the authors in English.

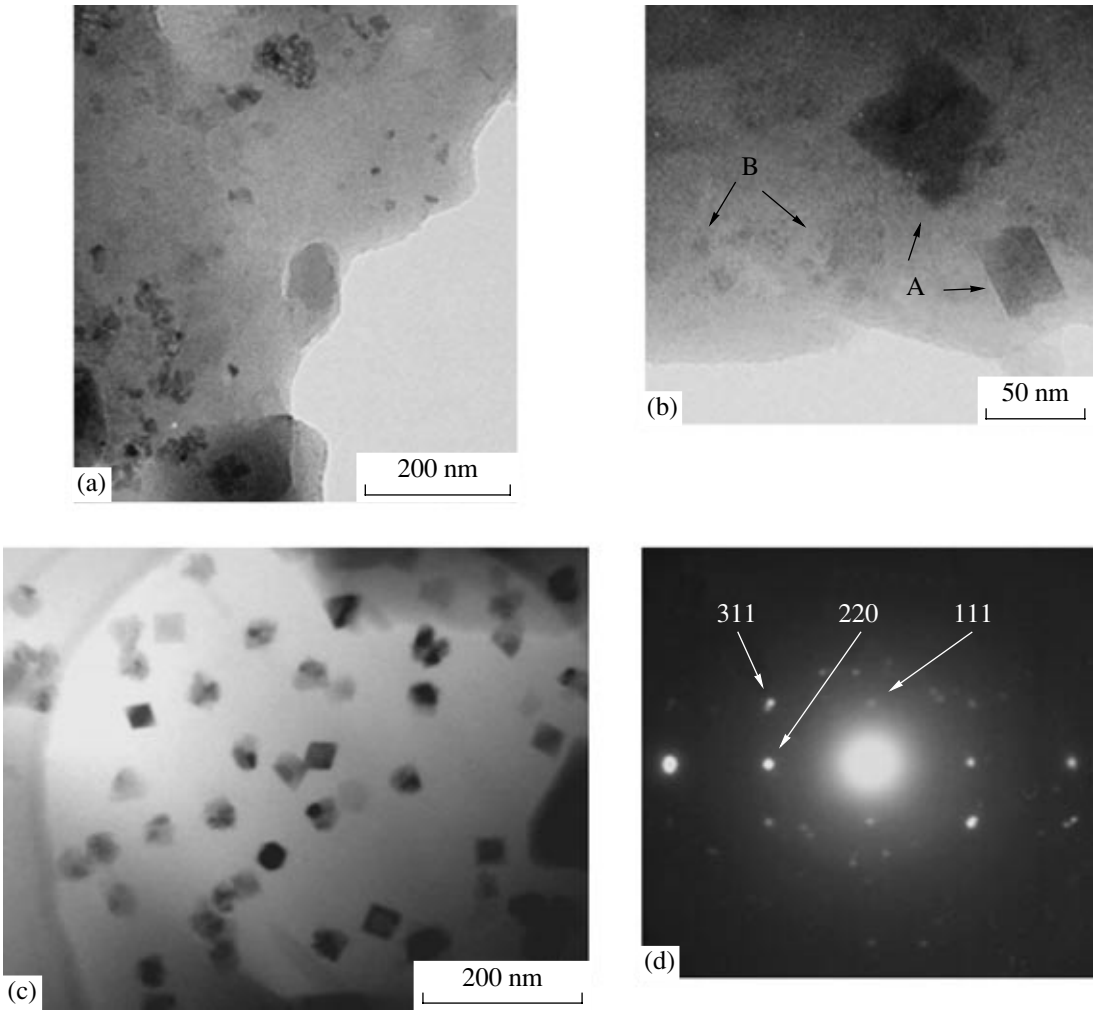

Fig. 1. HRTEM images for glasses (a) 1, (b) 2, and (c) 3; and (d) an electron diffraction pattern of ferrite particles marked by an arrow A in glass 2 in (b).

tor–analyzer (the limit of the element detection is ~10^{-3} μg/ml; and the errors, 3—5%). The particle size, shape, and crystal structure have been analyzed by HRTEM using a JEM-2010 device operating at 200 keV. Both the phase contrast method and electron microdiffraction were used with a locality of about 10 nm. Chemical analysis was performed in situ using energy dispersive X-ray analysis (EDXA) with a locality of 10–25 nm. The samples were prepared by grinding the glasses in ethanol and depositing them on Cu grids coated with thin amorphous carbon films. The Mössbauer spectra were obtained with a constant-acceleration Mössbauer spectrometer at room temperature with a ^{57}Co in Cr source of γ radiation. The spectrometer was calibrated using α-Fe_2O_3 as a standard. The static magnetic properties of glasses were measured at room temperature using a vibrating-sample magnetometer. FR was measured as a function of an external magnetic field. The plane-polarization modulation provided the accuracy of the FR measurements ±0.2 min. An external magnetic field was directed normal to the glass surface and changed from –5 to +5 kOe.

3. RESULTS AND DISCUSSION

The gross composition of glasses 1, 2, and 3 was determined chemically with ICP AES to be $K_{0.97}AlB_{2.78}Mn_{0.023}Fe_{0.042}$ with Mn/Fe = 0.54, $K_{1.06}AlB_{2.60}Mn_{0.048}Fe_{0.076}$ with Mn/Fe = 0.63, and $K_{1.04}AlB_{2.90}Mn_{0.036}Fe_{0.041}$ with Mn/Fe = 0.88, respectively. So, the molar ratio Mn/Fe in all the glasses exceeds 0.5, which is the ratio of the strictly stoichiometric ferrite $MnFe_2O_4$. This means that either a single-phase solid solution $Mn_{1+x}Fe_{2-x}O_4$ with $0.1 < x < 0.4$ or a mixture of $MnFe_2O_4$ and the manganese oxide are formed in these glasses.

An analysis of the XRD patterns indicates that glasses 2 and 3, similar to the analogous glass samples presented in [5], have the same cubic spinel structure and their peaks at $2\Theta = 35.2°$, ≈43°, and ≈56° correspond to those of the coarse $MnFe_2O_4$ powder. Glass 1

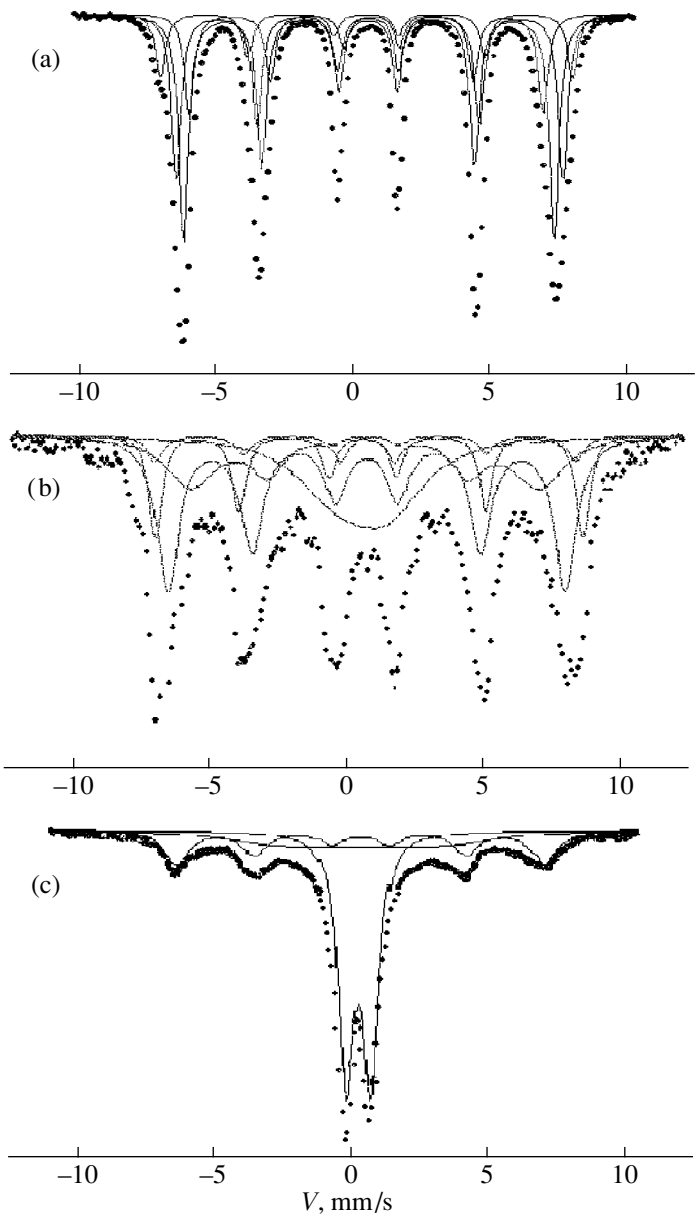

Fig. 2. Room-temperature Mössbauer spectra of (a) bulk $MnFe_2O_4$ crystals and of nanoparticles of (b) glass 3 and (c) glass 2.

does not exhibit diffraction peaks. The patterns of glasses 2 and 3 show broadening of all the peaks, reduction of intensity, and increase in the diffuse background as compared to the pattern of the coarse $MnFe_2O_4$ powder. This means that the ferrite crystallites in the glasses are not only small in size but are also disordered, most likely, defect, and even amorphous. The profile of the (311) peak ($2\Theta = 35.2°$) was used for the calculation of the ferrite-crystallite size (the coherent scattering range). According to the Scherrer formula, the average crystallite sizes were found to be ~250 Å for glasses 2 and 3. So, the X-ray diffraction study indicates the formation of ferrite particles in glasses 2 and 3, while in glass 1 the ferrite detection was outside the domain of XRD.

According to the DDA data, single-phase particles of $MnFe_2O_4$ and $Mn_{1.1}Fe_{1.9}O_4$ composition are formed in glasses 1 and 2, and the latter phase with an Mn excess is less stable against the heat-treatment temperature [8]. Particles of glass 3 are also close to stoichiometric ferrite, but the Mn and Fe oxides are present in the glass matrix in a dissolved state or as solid inclusions. For all the glasses, a spatial chemical heterogeneity is observed due to a slightly different composition of ferrite particles distributed in the matrix. One can also expect a different cation distribution between tetrahe-

dral and octahedral positions of the spinel lattice for these particles.

High-resolution TEM images of glasses 1–3 are illustrated in Fig. 1. The isolated particles of glass 3 are relatively uniform in size and they are quite evenly distributed in the matrix. On the other hand, HRTEM images of glasses 1 and 2 show polydisperse features in a lower-contrast matrix. In all the glasses, particles of 30–50 nm in size analyzed by electron diffraction and compared to the bulk $MnFe_2O_4$ could be identified as a ferrite with a cubic spinel structure [9], while the weak-contrast aggregated particles do not show diffraction spots. The presence of Mn and Fe in the fields of particles imaged by HRTEM was confirmed by EDXA. The composition of the large particles of glasses 3 and 2 was almost stoichiometric, while the composition of smallest particles of glasses 1 and 2 was non-stoichiometric; the Mn/Fe ratio in them was equal to 0.54 and 0.61, respectively. Besides, the composition of small particles of glass 2 was found to be enriched in Fe. It is known that the Mn excess in ferrite leads to a transfer of Fe from the core to the shell of particles, increasing the disorder of the surface ions [10]. The Mn and Fe disorder found by HRTEM correlates well with a non-uniform composition of the smallest particles observed by DDA through a variable value of the Mn/Fe ratio. It is interesting to note that the presence of Mn and Fe was detected by EDXA in the matrix field absolutely free from particles for glass 3. This indicates that these elements are present in the matrix in a dissolved state, which was observed also by the DD analysis.

The formation of ferrite particles in borate glasses was reliably established from XRD, DDA, and HRTEM data, but the size, shape, stoichiometry, and crystalline quality of the particles, remaining typical of the manganese ferrite, vary depending on the preparation conditions in fairly wide limits. The difference in the size of particles determined by HRTEM and calculated from XRD was explained due to the methodology difference between these techniques. The Mössbauer spectra of glasses 1–3 consist of the sum of Zeeman sextets and quadrupole doublets (Fig. 2). The analysis of the spectra was made by comparing them with the Mössbauer spectrum of the bulk single-crystal $MnFe_2O_4$ with a partly inverse spinel structure. Each spectrum was computer-fitted on the assumption of a minimum number of nonequivalent Fe positions. The results are collected in Table 1.

Based on the Mössbauer study, it was established that the ferrite particles possess a magnetic order, and this order is close to that of the bulk manganese ferrite at least for the large-size particles. Additionally, it was shown that the magnetic state (superparamagnetic or blocked) is correlated with the ferrite particle size. The difference between the spectra parameters of glasses 1–3 are associated with different Mn concentration in the ferrite particles, with the difference in the first neighbors of the metal ions taking part in magnetic interaction, and with small size of the ferrite particles.

Table 1. Mössbauer parameters of the bulk $MnFe_2O_4$ ferrite and glasses 3, 2, and 1: isomeric chemical shift δ (mm/s) relative to α-Fe, hyperfine field H_{hf} at the iron nucleus (kOe), quadrupole splitting ε (mm/s), and line half-width at half-maximum Γ (mm/s). The fitting error is 0.062

No.	δ	H_{hf}	ε	Γ	Location*
bulk	0.30	465	0	0.13	*A*
	0.40	436	0.12		B_1
	0.39	418	0.07		B_2
	0.40	398	–0.40		B_3
3	0.37	396	0	0.64	*A*
	0.39	402	–0.39	0.46	B_1
	0.41	373	0	0.82	B_2
	0.40	327	–0.18	0.44	B_3
	0.34	67	0.48	2.49	SPM
2	0.39	390	0	1.07	
	0.43	202	0.01	3.16	
	0.32	–	0.84	0.63	
1	0.42	233	0.25	5.07	
	0.37	–	0.91	0.79	

*Appearance of nonequivalent octahedral positions B_1 (4Mn2Fe), B_2 (5Mn1Fe), and B_3 (6Mn) in the partly inverse spinel is a well-known phenomenon associated with the different surroundings of [B] ions by magnetic ions of the second coordination shell [10].

The magnetization curves of glasses 1 and 3 are depicted in Figs. 3a and 3b, respectively. The high magnetic susceptibility, magnetic saturation in low magnetic fields, and magnetic hysteresis conclusively prove the ferri- or ferromagnetic behavior of the glasses. The values taken as the saturation magnetization M_s in the glasses change in the order 2 > 3 > 1 (Table 2). The M_s values of glasses 2 and 3 are quite close, while that of glass 1 differs from them almost by an order of magnitude. Three factors may explain the origin of the reduction of *M* in glasses: the amount of the ferrite phase itself, the size effect, the spin disorder in the particles with increasing *S*/*V* ratio, and the superparamagnetic-relaxation phenomenon. In the glass row 2 ⟶ 3 ⟶ 1, the amount of the ferrite phases varies as 5 > 3 > 2 (in wt %) according to the DD analysis; the average size of the particles varies as 5 to 30 ⟶ 50 ⟶ 5 nm according to XRD and HRTEM data; and a superparamagnetic relaxation exists in glass 3 according to the Mössbauer experiment. The influence of the particle shapes and of the shape of agglomerates on M_s is not quite clear, although the shape anisotropy was absent in all the glasses ($M_\perp \approx M_\parallel$, Table 2). The uniform and quite large size of ferrite particles of glass 3 allows the saturation magnetization to be estimated as ~50 emu/g,

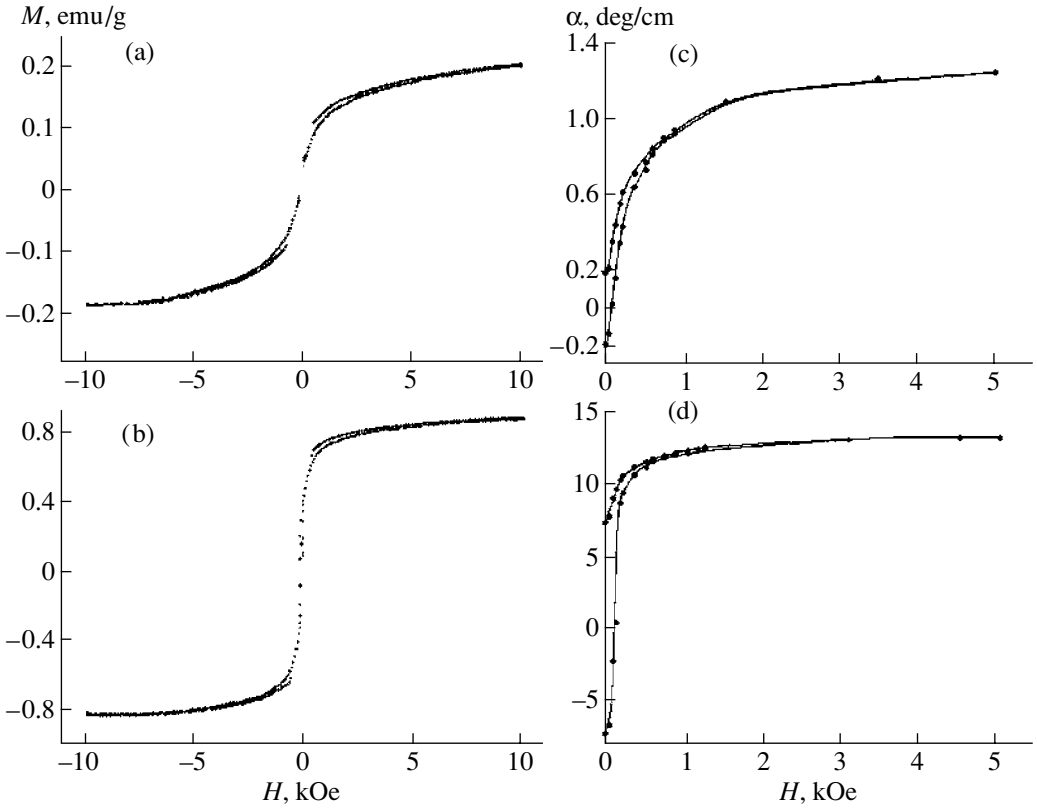

Fig. 3. (a, b) Magnetization curves measured as a function of field for glasses 1 and 3, respectively; (c, d) FR field dependences at $\lambda = 925$ nm for glasses 1 and 3, respectively.

which is close to that of bulk ferrite reported in the literature as 80 emu/g at room temperature [11]. The underestimated value of M in our case may be caused by the entering of some Al^{3+} ions into the ferrite lattice and/or by the spin disorder of paramagnetic ions due to structural defects and microdeformations of the particles with decreasing their size [12]. Owing to the higher FR-technique sensitivity, the FR field dependences allow one to obtain a more detailed description of the hysteresis loops in the low-field region. The loop of glass 3 (Fig. 3d) is almost rectangular with a remanent magnetization equal to half the M_s. The loop of glass 1 (Fig. 3c) implies that most particles are superparamagnetic, while some particles are blocked at room temperature according to a small value of the remanent magnetization. Therefore, one can suggest that the average particle size ~7 nm is the boundary between the superparamagnetic and blocked states of the ferrite particles of glass 1. The loop of glass 2 with the bimodal sizes of the particles occupies an intermediate position between the above curves. It is worth pointing to the high remanent FR value (α_r) for glass 3, which falls to approximately half the value of α in the saturated magnetic field. So, the sample could be considered as a transparent permanent magnet. As is seen from Table 2, an unusual peculiarity of the α/M ratio is observed at the same magnetic field. Being the same for glasses 2 and 3, it was much less for glass 1. The behavior like this seems to be strange because the FR has to be a linear function of M. One of the possible mechanisms that may explain the finding is a redistribution of Mn^{2+} and Fe^{3+} ions between octahedral and tetrahedral positions of the spinel structure. Having the same effective magnetic moment, these ions, when being redistributed in the lattice, do not change the total magnetization values. However, another situation takes place with the FR which is associated with the definite electron transitions and depends not only on the transition magneto-optical activity but also on the distance between the energy of this transition and the energy of the FR observation. The mechanism is considered in detail in [13].

Table 2. $M_\perp$ and $M_\parallel$ magnetizations at a magnetic field $H =$ 3.5 kOe perpendicular and parallel to the sample surface, respectively; specific Faraday rotation (α) in a 3.5-kOe perpendicular field, and the α/M ratio

No.	$M_\perp$, emu/g	$M_\parallel$, emu/g	α, deg/cm, $\lambda = 925$ nm	α/M
1	0.018	0.019	2.46	136.6
3	0.085	0.090	14.0	164.0
2	0.112	0.116	18.55	165.9

4. CONCLUSIONS

Nanosized ferrite particles can be successfully obtained by crystallization of K–Al–borate glasses. The final characteristics of particles, such as their size, shape, stoichiometry, and defect structure, show a wide variety when going from one glass to another, depending on the preparation conditions. A strong influence of these parameters on the magnetic behavior of the ferrite particles in the glasses was revealed. The results are very encouraging for the search of a general mechanism that determines the size, shape and nanostructure of the particles.

ACKNOWLEDGMENTS

This research was supported in part by the Integrated Project of the Siberian Division of the Russian Academy of Sciences no. 88-2003, and by the Federal Program RNP, project no. 2.1.1.7376.

REFERENCES

1. V. I. Skorospelova and S. A. Stepanov, Izv. Akad. Nauk SSSR, Neorg. Mater. **10**, 1864 (1974).
2. S. A. Stepanov, Fiz. Khim. Stekla **2**, 228 (1976).
3. I. Edelman et al., Physica B: Condens. Matter **301**, 203 (2001).
4. S. A. Stepanov et al., Optich. Zh. **70** (12), 46 (2003) [J. Opt. Tecnhol. **70**, 870 (2003)].
5. I. Edelman et al., Phys. Met. Metallogr. **91** (Suppl. 1), S116 (2001).
6. I. P. Suzdalev and P. I. Suzdalev, Usp. Khim. **70**, 203 (2001) Russ. Chem. Revs. **70**, 177 (2001)].
7. V. V. Malakhov, J. Mol. Catal. A: Chemical **158**, 143 (2000).
8. Y. D. Tretyakov, *Thermodynamics of Ferrites* (Khimiya, Leningrad, 1967) [in Russian].
9. Database PDF–2, JCPDS, no. 10–0319 (1997).
10. Ph. Tailhades, in *Nano-Crystalline and Thin Film Magnetic Oxides*, Ed. by I. Nedkov and M. Ausloss NATO Science Series **3**: High Technology (1972), p. 3.
11. J. Smit and H. P. J. Wijn, *Ferrites* (Philips Research Laboratories. N.V. Philips Gloeilampenfabrieken, Eindhoven, 1959).
12. R. H. Kodama and A. E. Berkowitz, Phys. Rev. B **59**, 6321 (1999).
13. R. D. Ivantsov et al., Phys. Met. Metallogr. **100** (Suppl. 1), 97 (2005).